Heliyon 9 (2023) e22991

Contents lists available at ScienceDirect

Heliyon

journal homepage: www.cell.com/heliyon

Development and implementation of natural killer cell simultaneous ADCC and direct killing assay

Maia M.C. Bennett-Boehm [a,b,1], Anna R. Mahr [a,1], Sean T. Hartwell [a], Alexander K. Regan [a], Isabelle S. Weber [a], Arriana Blackmon [a], Cami R. Bisson [a], Angela N. Truong [a], Bella A. Circo [a], Jaden Nienhueser [a], Donald R. Rogers [a], Nathan Booher [a], Nithya Rajagopalan [a], Jacob W.S. Martens [a], Paul W. Denton [a,*]

[a] Department of Biology, University of Nebraska at Omaha, Omaha, Nebraska, USA
[b] Department of Information Science and Technology, University of Nebraska at Omaha, Omaha, Nebraska, USA

ARTICLE INFO

Keywords:
NK cell
Killing assay
ADCC
Direct killing
Flow cytometry
Immunophenotype

ABSTRACT

Assays to quantify natural killer (NK) cell killing efficacy have traditionally focused on assessing either direct killing or antibody dependent cell-mediated cytotoxicity (ADCC) independently. Due to the probability that immunotherapeutic interventions affect NK cell-mediated direct killing and NK cell-mediated ADCC differently, we developed an assay with the capacity to measure NK cell-mediated direct killing and ADCC simultaneously with cells from the same human donor. Specifically, this design allows for a single NK cell population to be split into several experimental conditions (e.g., direct killing, ADCC), thus controlling for potential confounders associated with human-to-human variation when assessing immunotherapy impacts. Our Natural Killer cell Simultaneous ADCC and Direct Killing Assay (NK-SADKA) allows researchers to reproducibly quantify both direct killing and ADCC by human NK cells. Furthermore, this optimized experimental design allows for concurrent analysis of the NK cells via flow cytometric immunophenotyping of NK cell populations which will facilitate the identification of relationships between NK cell phenotype and the subsequent killing potential. This assay will be valuable for assessing the broader impact(s) of immunotherapy strategies on both modes of NK cell killing.

1. Introduction

NK cells share similar functions to cytotoxic T cells, but do not require prior antigen exposure to gain cytotoxic function [1]. NK cells are not exclusively cytotoxic in nature, as they progress through a maturation spectrum from cytokine production to cytotoxicity marked largely by the expression of the canonical NK cell markers CD56 and CD16. Cytokine-producing $CD56^{bright}CD16^{dim/neg}$ NK cells function largely in response to receptor activation or extracellular cytokine signaling and aid in progressing various immune responses. Post-NK cell activation, the production of inflammatory cytokines such as interferon gamma (IFN-γ) and tumor necrosis factor alpha (TNF-α) [2]. These signaling molecules help to activate other immune cells, enhancing the immune response. Cytotoxic $CD56^{dim}CD16^{pos}$ NK cells target and kill diseased cells by one of two known mechanisms: direct killing or antibody dependent

* Corresponding author.
E-mail address: pdenton@unomaha.edu (P.W. Denton).
[1] Equal contributing first authors.

https://doi.org/10.1016/j.heliyon.2023.e22991
Received 13 July 2023; Received in revised form 9 November 2023; Accepted 23 November 2023
Available online 28 November 2023

cell-mediated cytotoxicity (ADCC). Direct killing relies on "missing-self" signals from target cells lacking MHC-I on their surface. The lack of an inhibitory signal through MHC-I allows the NK cell to recognize the target cell as pathogenic or diseased [3]. ADCC relies on the incorporation of a target cell specific antibody to bridge the NK cell and the target cell when the target cell retains MHC-I on its surface. Certain malignancies (e.g., B cell lymphoma) retain MHC-I on the cells' surface and would go undetected by NK cells without the use of an ADCC antibody (e.g., rituximab) [4,5]. Due to these multifaceted functions, NK cells have become targets for immunotherapeutic interventions with the intention of harnessing and enhancing their ability to kill diseased cells.

Prior to clinical implementation, immunotherapies are evaluated using methods such as cell-based killing assays. Killing assays determine how effectively various immune cells kill diseased cells post-therapy exposure. These assays are crucial tools typically used to facilitate the understanding of how an indicated molecule (e.g., immunotherapies) impacts specific cell populations *ex vivo* prior to *in vivo* utilization. There exist many methodologies by which researchers can study how therapeutics impact individual cell populations (e.g., NK cells, cytotoxic T cells) or pools of cells (e.g., PBMCs) in both human and murine environments [e.g. Refs. [6–9]]. In these contexts, NK cell-mediated killing assays have traditionally focused on one method of NK cell-mediated killing, either direct killing or ADCC.

The implementation of an assay focusing on one method of killing may lead to the assumption that the discoveries made using each method (e.g., direct killing or ADCC) would apply to the other. To avoid such assumptions, we hypothesized that it was feasible to develop an NK cell-mediated killing assay which combines the two known methods of NK cell-mediated killing: direct killing and antibody dependent cell-mediated cytotoxicity (ADCC). Using such an approach, it would be possible to assess both forms of killing with a single human donor so that relationships between both killing outcomes could be systematically and quantitatively assessed rather than assumed. To develop such an assay, we incorporated existing procedures from traditional NK cell-mediated assays, including flow cytometry-based data acquisition, with multiple optimizations to allow for a greater number of experimental variables to be tested [e.g. Refs. [10–14]]. Our novel approach, the Natural Killer cell Simultaneous ADCC and Direct Killing Assay (NK-SADKA), allows for the reproducible quantification of the impacts of immunotherapies, or other experimental variables, on both methods of NK cell-mediated killing simultaneously while controlling for human-to-human variation present between donors.

2. Methods

2.1. Blood product procurement

Blood products (i.e., buffy coats) from deidentified human donors were procured by the American Red Cross. PBMCs were purified using Ficoll-Paque density gradient centrifugation (Beckman Coulter; 470×*g*, 25 min, 20 °C, 5/10 acceleration, 1/10 deceleration) [10]. PBMCs were then resuspended in RPMI 1640 medium (ATCC, cat# 30–2001) supplemented with 10 % fetal bovine serum (FBS) (Avantor, cat# 97068-065) and 1 % penicillin/streptomycin (VWR, cat# 21J195302) (cRPMI-10) and 5 Units/mL DNase I (Roche Diagnostics, cat# 04716728001) at 10×10^6 cells/mL. Cells were then aliquoted into six well plates (Sarstedt, cat# 83.3920) at 5×10^6/mL in 5 mL per well. All plates were incubated at 37 °C with 5 % CO_2 for ~60 h to accommodate immunotherapeutic testing not further discussed herein. An overnight incubation can be used if extended drug treatments are not warranted.

2.2. Target cells

Human Burkitt's lymphoma (Daudi) cells (CCL-213, ATCC) [15] were cultured in RPMI 1640 medium (ATCC, cat# 30–2001) supplemented with 20 % FBS and 1 % penicillin/streptomycin (cRPMI-20). Human chronic myelogenous leukemia (K562) cells (CCL-243, ATCC) [16] were cultured in Iscove's Modified Dulbecco's Medium (IMDM) (Corning, cat# 10-016-CV) supplemented with 10 % FBS and 1 % penicillin/streptomycin (cIMDM-10). Both cell lines were incubated at 37 °C with 5 % CO_2. Daudi and K562 cells were passaged approximately every 48 h. Each passage was accomplished by reseeding 3×10^6 cells (Daudi) and 1×10^6 cells (K562) in 9 mL of their respective media plus 1 mL of conditioned media that was retained from the previous passage. Cells were used as target cells in killing assays between 5 and ~25 passages.

2.3. NK cell magnetic enrichment

Human NK cells were enriched using a Human NK Cell Isolation Kit (Miltenyi Biotec, order #130-092-657) according to the manufacturer's instructions [10]. Briefly, degassed phosphate buffered saline (PBS) supplemented with 0.5 % bovine serum albumin (BSA) (Roche, cat# 03-117-332-001) and 2 mM EDTA (VWR, cat# AC327345000) (MACS buffer) and Biotin Antibody Cocktail (cat# 5220509658) were added to whole PBMC samples. The resulting solution was mixed (via pipetting) and incubated (4 °C, 5 min). Additional MACS buffer and Human NK Cell Microbeads (Miltenyi Biotec, cat# 5220509658) were added and mixed (via pipetting), then incubated (4 °C, 10 min). The QuadraMACS magnet (Miltenyi Biotec, order #130-090-976) was assembled with LD columns (Miltenyi Biotec, order #130-042-901) and pre-separation filters (Miltenyi Biotec, order #130-095-823), which were prewashed with 6 mL of MACS buffer. PBMCs were pipetted into columns at less than 70 % of maximum column capacity. Once samples completely passed through the column, two consecutive washes of 3 mL of MACS buffer were each were completed. Negative fractions (i.e., NK cell containing fractions) were centrifuged (350×*g*, 15 min, 20 °C) and pellets were resuspended in 1 mL of RPMI 1640 no phenol red medium (Quality Biological, cat# 112-040-101) supplemented with 10 % FBS and 1 % penicillin/streptomycin (cRPMI-NPR) and counted using trypan blue exclusion. The use of NPR media mitigates the potential risk for phenol red interfering with flow cytometric analysis.

2.4. Target cell staining

Daudi and K562 cells were resuspended separately in PBS and incubated with 1.2 μM 5(6)-Carboxyfluorescein diacetate n-hydrosuccinimide ester (CFDA-SE; cat# 75003, Stemcell Technologies) for 3 min at 37 °C with a 1:1 (cell volume: stain volume) ratio. Cell staining was quenched via the addition of 2 mL cRPMI-NPR followed by an incubation for 10 min at 37 °C and 5 % CO_2. Samples were centrifuged (350×*g*, 15 min, 20 °C), supernatant aspirated, and pellet resuspended in 10 mL PBS. This sample then centrifuged a second time (350×*g*, 15 min, 20 °C) to remove all residual CFDA-SE. Supernatants were aspirated, and cells were resuspended at a concentration of 2×10^5 cells/mL in cRPMI-NPR.

2.5. Co-incubation of assay components

Previously enriched NK cells and stained target cells were aliquoted into sterile 5 mL round-bottom polypropylene test tubes (Fisher Scientific, cat# 14-959-1B) at a 5:1 NK to target cell ratio. α-CD20 (rituximab; Selleck Chemical, #A20095MG) was added to ADCC samples at a dosage of 4 μL per 1 mL media. Samples were covered loosely with aluminum foil and incubated at 37 °C with 5 % CO_2 for the indicated time frame.

2.6. Cell staining for flow cytometric analyses

Post incubation, samples were centrifuged (350×*g*, 15 min, 20 °C), the supernatant decanted, and the cells were vortexed briefly to disrupt the pellet. For killing assessment, 10 μL of 7-aminoactinomycin D (7-AAD) (Stemcell, cat #75001) was added to the samples in the approximately 100 μL of residual supernatant, vortexed gently to mix, and samples were incubated for 10 min at 20 °C in the dark. Separately, for immunophenotypic analysis, samples were centrifuged (350×*g*, 15 min, 20 °C) following the 2-h incubation. Then, the supernatants were decanted, and cells were vortexed briefly to disrupt the pellet. Samples were then blocked with 5 μL human FcX block (cat#422302; 10 min). Following this, samples were stained (15 min) with the following flow cytometry antibodies: a lineage cocktail (anti-CD3, anti-CD14, anti-CD19), anti-CD16, and anti-CD56 (Table 1) [10,17–21]. PBS was added to sample tubes for a final volume of 3 mL. Samples were centrifuged (350×*g*, 15 min, 20 °C), the supernatant decanted, and cells vortexed briefly to disrupt the pellet. 5 μL 7-AAD was then added to the samples resuspended in approximately 100 μL of residual supernatant. Samples were vortexed and incubated for 10 min at 20 °C in the dark. Following incubation, samples were ready for flow cytometry.

2.7. Flow cytometric analyses

Flow cytometry data were collected using a Beckman Coulter CytoFLEX flow cytometer and analyzed with FlowJo v10.8.2 (BD). NK cell purity was assessed based on the percentage of Lineage^{neg} (CD3, CD14, CD19) and CD56^{pos} cells post-magnetic isolation. For killing determination, target cell death was established as the percentage of 7-AAD^{pos} cells in the total CFSE^{pos} population (stained target cells). NK cell killing efficacy for ADCC and direct assays is determined by the general formula: ***killing efficacy = % target cell death (experimental) - % target cell death (control)***. For immunophenotyping, Lineage^{pos} and 7-AAD^{pos} cells were excluded. NK cells were established as Lineage^{neg} CD56^{pos}.

3. Results

3.1. Optimized effector and target cell preparation facilitates flow cytometric discrimination of NK cells from target cancer cells

We began by isolating human PBMCs and then magnetically enriching NK cells from those PBMCs following an incubation (Fig. 1A). Simultaneous to the NK cell magnetic enrichment, target cells (Daudi and K562) were stained with CFDA-SE. This molecule becomes the fluorescent stain CFSE when cleaved upon diffusion into the cell and was herein used for discriminating between unstained effectors (NKs) and stained targets in flow cytometric analyses (Fig. 1B). PBMC yields following density centrifugation were ~2×10^9 PBMCs (Fig. 1C) and NK cell magnetic enrichment yields exhibited ~90 % NK cell purity (Fig. 1D). It was necessary to determine a concentration of CFDA-SE with a mean fluorescent intensity (MFI) substantially higher than that of unstained cells, but low enough to limit spillover into the channel where the live/dead discriminator 7-AAD is detected (PC5.5). During titration of CFDA-SE concentration in each target cell type, we found that staining with 1.2 μM CFSA-SE resulted in a ~1.5 log separation of the negative

Table 1
Reagents utilized for NK cell surface flow cytometric analyses.

Marker	Clone	Fluorophore	Purpose	Catalog
CD3	UCTH1	FITC	Lineage exclusion (T cells)	BioLegend #300406
CD14	HCD14	FITC	Lineage exclusion (macrophages, monocytes, granulocytes)	BioLegend #325604
CD19	HIB19	FITC	Lineage exclusion (B cells)	BioLegend #302206
CD56	HCD56	APC	Consensus NK cell marker	BioLegend #318310
CD16	3G8	Pacific Blue	NK cell marker, ADCC mediator	BioLegend #302032
–	–	7-AAD	Live/dead discriminator	Stem Cell Tech# 75001

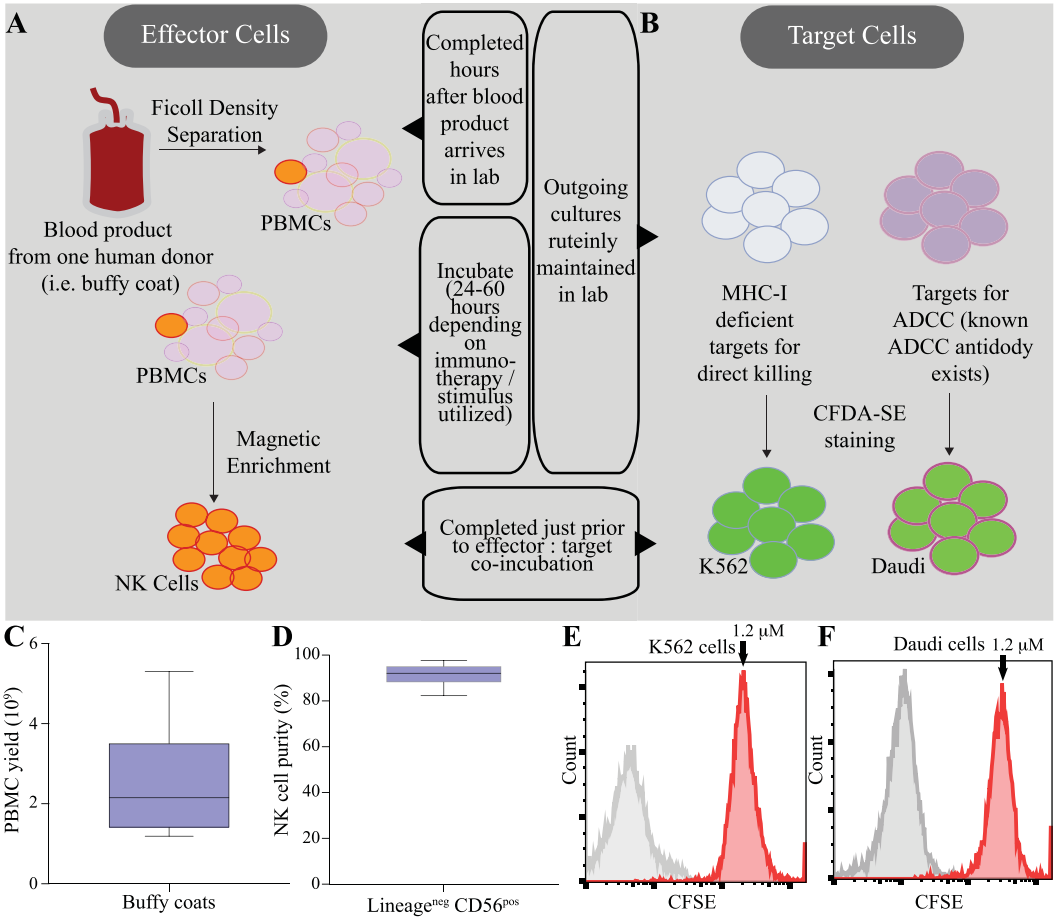

Fig. 1. Effector and target cell preparation steps. (A–B) Schematic depicts PBMC isolation from blood product via density centrifugation, PBMCs incubation, and NK cells magnetic enrichment **(A)** as well as target cell staining using CFDA-SE (1.2 µM) **(B). (C)** PBMC yields after Ficoll density centrifugation (n = 26). **(D)** NK cell purity based on Lineage^{neg}CD56^{pos} population in flow cytometric analyses performed post-magnetic enrichment (n = 20). **(E–F)** Representative histograms of CFSE fluorescence in K562 cells **(E)** and Daudi cells **(F)**. Grey histograms represent unstained control and red histograms represent 1.2 µM CFDA-SE (CFSE) staining – the optimal concentration for discrimination between unstained/stained K562 and Daudi cells while minimizing spill over into the viability channel.

and positive peaks (Fig. 1E–F) with minimal spillover into the channel detecting 7-AAD.

3.2. Optimized coincubation conditions minimizes required cell yields and time allocation while preserving killing efficacy

After target cells were stained and NK cells were enriched from the total PBMC population, effector and target cells were combined as described in the methods for the co-incubation period (Fig. 2A–B). Our optimal effector-to-target ratio was determined by comparing 5:1 and 10:1. We sought to use the ratio which allowed for the least number of effector (NK) cells to allow for more conditions to be tested. Due to the minimal differences in outcomes between 5:1 and 10:1, effector-to-target ratios, for both target cell lines (Fig. 2C–D), we adopted a 5:1 effector-to-target ratio. The incubation times were examined along with the effector-to-target ratios. For this, we tested both 2 h and 4 h. There was minimal difference between the two conditions (Fig. 2C–D). Therefore, the shorter 2-h time was adopted for efficiency. Thus, the 5:1 effector-to-target ratio and 2-h incubation time became our standard conditions.

To bridge NK and Daudi cells in ADCC, rituximab [5,22] was used as the ADCC antibody. We titrated the antibody to determine whether there was a detrimental effect of rituximab on the target cells (Daudi) when no effector cells were present. We tested five concentrations of rituximab (5 mg/mL stock concentration; tested using 1, 2, 4, 6, and 8 µL per 1 mL cRPMI-npr). Regardless of the antibody concentration, rituximab alone was not cytotoxic to Daudi cells in the absence of NK cells. To ensure that sufficient ADCC antibodies were present in ADCC assays, we adopted 4 µL of rituximab per 1 mL as our working concentration in ADCC assays.

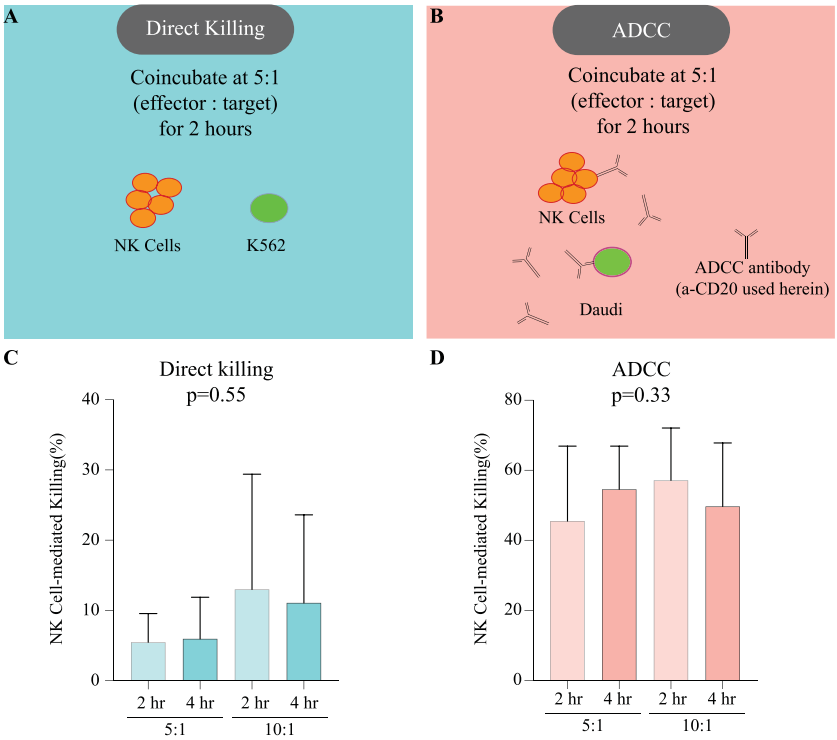

Fig. 2. Efficient direct killing and ADCC was observed with 2-h co-incubation at a 5:1 effector-to-target ratio. (A–B) Schematic detailing the co-incubation conditions in direct killing **(A)** and ADCC **(B)**. **(C–D)** NK cell killing efficacy expressed as a percentage for four different co-incubation conditions: 2-h co-incubation/5:1 ratio; 4-h co-incubation/5:1 ratio; 2-h co-incubation/10:1 ratio; 4-h co-incubation/10:1 ratio for direct killing **(C)** and ADCC **(D)**. Data presented as mean ± SEM.

3.3. Optimized assay conditions facilitate flow cytometric detection and analysis of NK cell-mediated killing efficacy

For data collection, 7-AAD (viability marker) was added to each coculture for live/dead discrimination. Post flow cytometric analysis, singlet lymphocyte events were analyzed to assess NK cell killing efficacy (Fig. 3A). For killing determination, CFSE and 7-AAD positive gates were used to determine percentage of dead target cells. After this percentage is determined (Fig. 3B), killing efficacy can be calculated (Fig. 3C) by subtracting control death from the experimental death depending on the specific conditions for direct killing (Fig. 3D) and ADCC (Fig. 3E).

3.4. Development of the NK-SADKA assay for simultaneous direct and ADCC surveillance enables further insights while mediating human-human variability

All of the above steps were combined into the NK-SADKA (Fig. 4). While retaining all the initial assay optimizations (Fig. 4A–E), we split the magnetically enriched NK cell population into two populations for the co-incubations (Fig. 4C–D). The NK-SADKA shows consistent ability to detect both direct killing and ADCC (Fig. 4F–G).

3.5. Implementation of the optimized NK-SADKA enables immunophenotyping and identification of canonical NK cell subsets in NK-SADKA samples

In minimizing the cell yield necessary to successfully run an NK-SADKA killing assay, the NK-SADKA optimizations also allow for separate NK cell immunophenotyping (Fig. 5A–C). With this NK cell immunophenotyping panel we could identify canonical cytokine-producing ($CD56^{bright}CD16^{dim/neg}$) and cytotoxic NK cells ($CD56^{dim}CD16^{pos}$). When analyzed by CD56 surface levels (bright vs. dim), we observed a predicted decrease in CD16 surface levels on $CD56^{dim}$ cells following killing (Fig. 5C) [23–25].

4. Discussion

Here we present a novel approach that allows for simultaneously assessing both direct killing and ADCC by human NK cells. Our starting point was to consider strategies described for either direct killing [7,9,26] or ADCC [27–29]. Building on these prior efforts, we moved forward with CFDA-SE staining of target cells and proceeded to optimize our experiments for both forms of killing in the joint

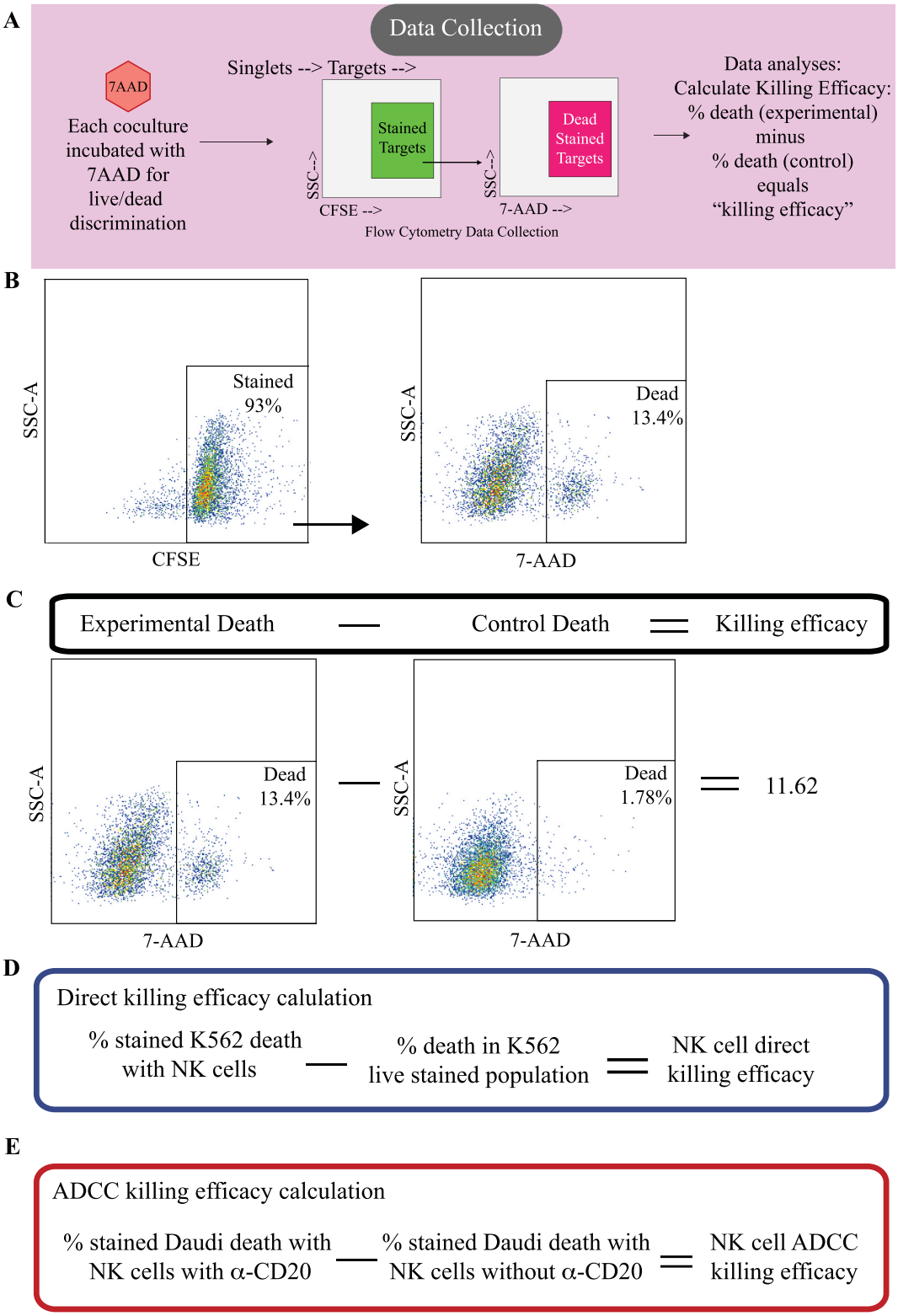

Fig. 3. Data collection via flow cytometric analyses. (A) Schematic detailing the application of 7-AAD live/dead discriminator, gating strategy used in data acquisition, and simplistic equation used to calculate NK cell-mediated killing efficacy. **(B)** Representative flow plots of stained target and dead target gates. **(C)** Equation for killing efficacy calculation with representative flow plots depicting the differences between experimental and control death populations. **(D–E)** The specific equations used for killing efficacy calculation in direct killing **(D)** and ADCC **(E)** are shown.

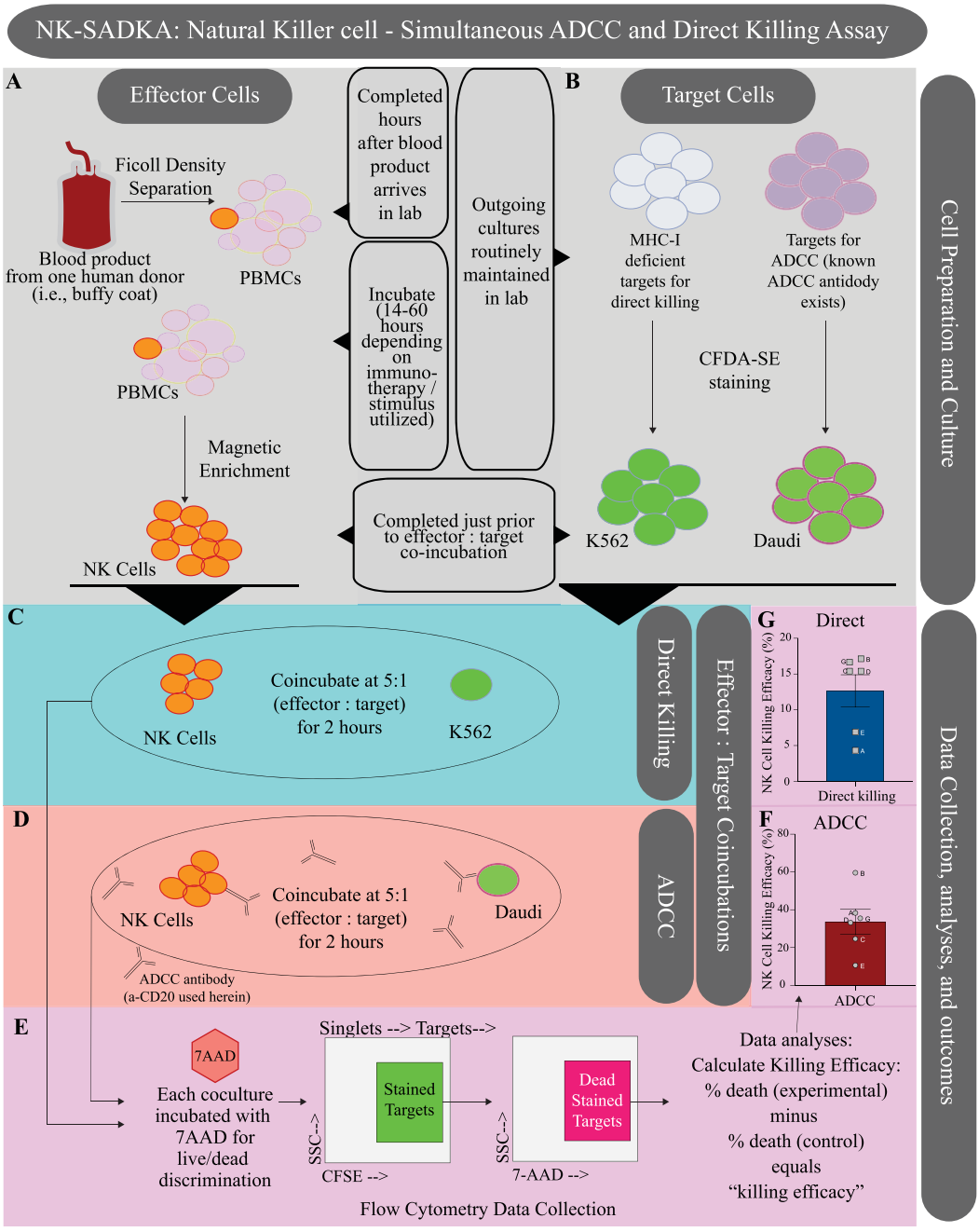

Fig. 4. Schematic detailing novel Natural Killer cell Simultaneous ADCC and Direct Killing Assay (NK-SADKA). (A) PBMC isolation from blood product via density centrifugation, PBMCs incubation, and NK cells magnetic enrichment **(A)** and target cell staining using CFDA-SE (1.2 μM) **(B). (C–D)** NK cell population split for co-incubation of effectors and targets. K562 cells used in direct killing **(C)** and Daudi cells used in ADCC **(D)** cells (5:1 ratio for 2 h). anti-CD20 antibody added for the ADCC condition. **(E)** Flow cytometric analysis conducted for NK killing efficacy determination. General equation detailed here with specific equation detailed in Fig. 3E–F. **(F–G)** Killing efficacy data are presented showing that both killing modalities can be measured using cells from the same human in a reproducible manner. Letters next to data points indicate unique human donors.

assay. Based on titration of the CFDA-SE proliferative dye, a concentration was determined that proved to be optimal for our use (i.e., 1.2 μM). In our context, optimal is defined as allowing for effective differentiation of target and effector cells while maintaining minimal spillover into the PC5.5 (7-AAD) channel. We also optimized the co-incubation conditions regarding the effector-to-target ratio and the duration of the co-incubation of effector and target cells. Due to the minimal difference between the levels of target cell death post co-incubation between the effector-to-target ratios and incubation durations, we moved ahead with conditions which

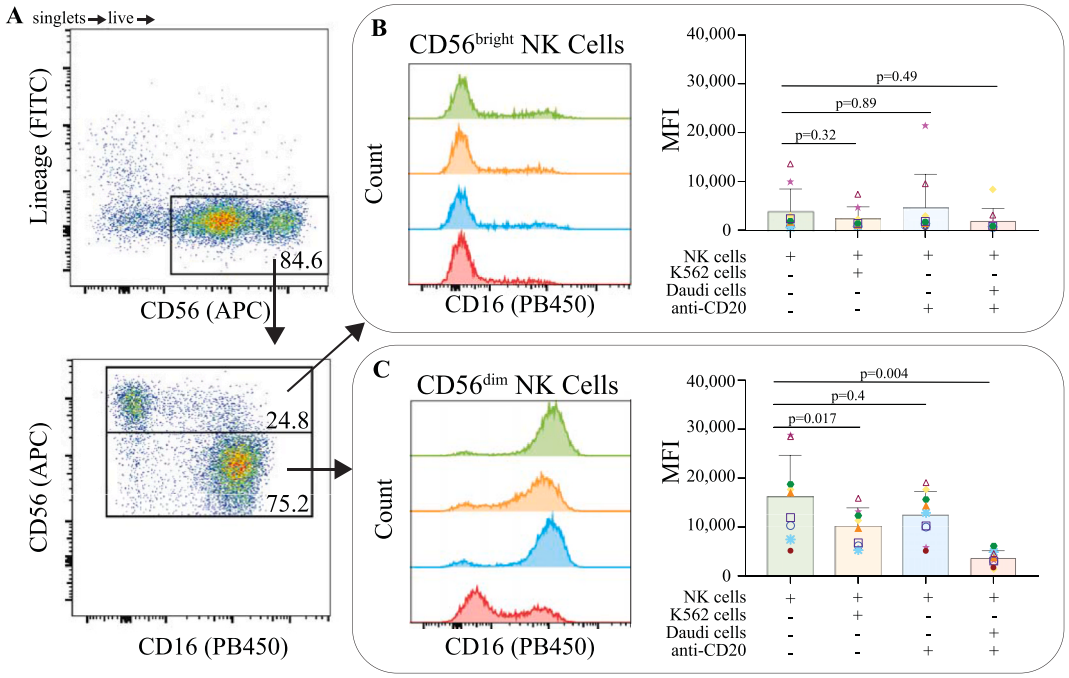

Fig. 5. NK-SADKA strategy allows for successful surface immunophenotyping. (A) NK cells were defined as Lineage^{neg} [CD3, CD14, CD19 (FITC)] and CD56^{pos}. Then this population was further defined as CD56^{bright} and CD56^{dim}. **(B–C)** CD56^{bright} **(B)** and CD56^{dim} **(C)** populations was then examined for CD16 mean fluorescence intensity (MFI) under four incubation conditions. Each dot represents an individual human sample. Statistical analyses: Mixed Effects Model (REML) with Dunnett's multiple comparisons test. Error bars represent SD.

conserve both time and resources – the latter allowing for an increase in the number of experimental variables that can be tested per donor. Furthermore, direct killing and ADCC levels were both robust and reproducibly quantifiable without being so high as to severely limit the dynamic range of the NK-SADKA for quantifying changes in NK cell killing capacity caused by various immunotherapy interventions. This was a critical outcome given that our primary goal for this assay was the evaluation of immunotherapy strategies. Finally, the scaling of the NK-SADKA facilitates simultaneous immunophenotyping of the NK cells which yielded expected outcomes that support that findings using the NK-SADKA are physiologically relevant.

In conclusion, the NK-SADKA is an efficient and effective assay for the quantification of NK cell-mediated direct killing and ADCC that controls for potential confounders associated with human-to-human variation.

Funding

PWD [as a developmental research project program (DRPP) investigator] and MMCBB, CRB, and ANT (as INBRE scholars) were supported by the National Institute of General Medical Sciences of the National Institutes of Health under award P20 GM103427. PWD is supported by the National Institute of Allergy and Infectious Diseases of the National Institutes of Health under award 1R15 AI178516. MMCBB, AB, and BAC were supported by University of Nebraska at Omaha Fund for Undergraduate Scholarly Experience (FUSE) funding. ARM was supported by University of Nebraska at Omaha Graduate Research and Creative Activity (GRACA) funding. PWD was supported by the University of Nebraska Collaboration Initiative (NR-26797). PWD was supported by startup funding from the University of Nebraska at Omaha. None of the specific sources of funding had any role in the conceptualization, design, data collection, analysis, decision to publish, or preparation of the manuscript.

Data availability statement

The datasets analyzed during this study are available from the corresponding author upon reasonable request.

CRediT authorship contribution statement

Maia M.C. Bennett-Boehm: Conceptualization, Data curation, Formal analysis, Funding acquisition, Investigation, Methodology, Writing - original draft, Writing - review & editing, Visualization. **Anna R. Mahr:** Conceptualization, Data curation, Formal analysis, Funding acquisition, Investigation, Methodology, Visualization, Writing - original draft, Writing - review & editing. **Sean T. Hartwell:** Data curation, Investigation, Methodology, Writing - review & editing. **Alexander K. Regan:** Data curation, Formal analysis, Investigation, Writing - review & editing. **Isabelle S. Weber:** Data curation, Formal analysis, Investigation, Visualization, Writing - review &

editing. **Arriana Blackmon:** Data curation, Investigation, Methodology, Writing - review & editing, Funding acquisition. **Cami R. Bisson:** Data curation, Investigation, Writing - review & editing, Methodology. **Angela N. Truong:** Data curation, Investigation, Methodology, Writing - review & editing. **Bella A. Circo:** Conceptualization, Investigation, Methodology, Writing - review & editing. **Jaden Nienhueser:** Data curation, Investigation, Methodology, Writing - review & editing. **Donald R. Rogers:** Data curation, Investigation, Methodology, Writing - review & editing. **Nathan Booher:** Data curation, Investigation, Methodology, Writing - review & editing. **Nithya Rajagopalan:** Data curation, Investigation, Methodology, Writing - review & editing. **Jacob W.S. Martens:** Data curation, Investigation, Methodology, Writing - review & editing. **Paul W. Denton:** Conceptualization, Data curation, Formal analysis, Funding acquisition, Investigation, Methodology, Project administration, Resources, Supervision, Validation, Visualization, Writing - original draft, Writing - review & editing.

Declaration of competing interest

The authors declare the following financial interests/personal relationships which may be considered as potential competing interests:Paul W Denton reports financial support was provided by National Institutes of Health. Paul W Denton reports financial support was provided by University of Nebraska Omaha. Paul W Denton reports financial support was provided by Nebraska Collaboration Initiative. Maia MC Bennett reports financial support was provided by National Institutes of Health. Maia MC Bennett reports financial support was provided by University of Nebraska Omaha. Cami R Bisson reports financial support was provided by National Institutes of Health. Angela N Truong reports financial support was provided by National Institutes of Health. Arriana Blackmon reports financial support was provided by University of Nebraska Omaha. Bella Circo reports financial support was provided by University of Nebraska Omaha. Anna Mahr reports financial support was provided by University of Nebraska Omaha.

Acknowledgements

The authors thank the American Red Cross for supplying blood products for this study.

References

[1] R. Kiessling, et al., "Natural" killer cells in the mouse. II. Cytotoxic cells with specificity for mouse Moloney leukemia cells. Characteristics of the killer cell, Eur. J. Immunol. 5 (2) (1975) 117–121, https://doi.org/10.1002/eji.1830050209.
[2] E. Vivier, et al., Innate or adaptive immunity? The example of natural killer cells, Science 331 (6013) (2011) 44–49, https://doi.org/10.1126/science.1198687.
[3] J.M. Elliott, W.M. Yokoyama, Unifying concepts of MHC-dependent natural killer cell education, Trends Immunol. 32 (8) (2011) 364–372, https://doi.org/10.1016/j.it.2011.06.001.
[4] G. Hashimoto, et al., Antibody-dependent cell-mediated cytotoxicity against influenza virus-infected cells, J. Infect. Dis. 148 (5) (1983) 785–794, https://doi.org/10.1093/infdis/148.5.785.
[5] G.J. Weiner, Rituximab: mechanism of action, Semin. Hematol. 47 (2) (2010) 115–123, https://doi.org/10.1053/j.seminhematol.2010.01.011.
[6] F. Kandarian, et al., A flow cytometry-based cytotoxicity assay for the assessment of human NK cell activity, J. Vis. Exp. 126 (2017), https://doi.org/10.3791/56191.
[7] J. Kim, et al., A flow cytometry-based whole blood natural killer cell cytotoxicity assay using overnight cytokine activation, Front. Immunol. 11 (2020) 1851, https://doi.org/10.3389/fimmu.2020.01851.
[8] P. Wong, et al., Flow cytometry-based ex vivo murine NK cell cytotoxicity assay, STAR Protoc 2 (1) (2021), 100262, https://doi.org/10.1016/j.xpro.2020.100262.
[9] X. Wu, et al., Improvements in flow cytometry-based cytotoxicity assay, Cytometry 99 (7) (2021) 680–688, https://doi.org/10.1002/cyto.a.24242.
[10] R. Offersen, et al., A novel Toll-like receptor-9 agonist, MGN1703, enhances HIV-1 transcription and NK cell-mediated inhibition of HIV-1 infected autologous CD4+ T-cells, J. Virol. 90 (9) (2016) 4441–4453, https://doi.org/10.1128/jvi.00222-16.
[11] H.H. van Ojik, et al., CpG-A and B oligodeoxynucleotides enhance the efficacy of antibody therapy by activating different effector cell populations, Cancer Res. 63 (17) (2003) 5595–5600.
[12] J.E. Wooldridge, et al., Immunostimulatory oligodeoxynucleotides containing CpG motifs enhance the efficacy of monoclonal antibody therapy of lymphoma, Blood 89 (8) (1997) 2994–2998.
[13] L. Fischer, et al., The anti-lymphoma effect of antibody-mediated immunotherapy is based on an increased degranulation of peripheral blood natural killer (NK) cells, Exp. Hematol. 34 (6) (2006) 753–759, https://doi.org/10.1016/j.exphem.2006.02.015.
[14] J. Golay, et al., Rituximab-mediated antibody-dependent cellular cytotoxicity against neoplastic B cells is stimulated strongly by interleukin-2, Haematologica 88 (9) (2003) 1002–1012.
[15] E. Klein, et al., Surface IgM-kappa specificity on a Burkitt lymphoma cell in vivo and in derived culture lines, Cancer Res. 28 (7) (1968) 1300–1310.
[16] C.B. Lozzio, B.B. Lozzio, Human chronic myelogenous leukemia cell-line with positive Philadelphia chromosome, Blood 45 (3) (1975) 321–334.
[17] S.M. Poznanski, A.A. Ashkar, What defines NK cell functional fate: phenotype or metabolism? Front. Immunol. 10 (2019) 1414, https://doi.org/10.3389/fimmu.2019.01414.
[18] A.M. Abel, et al., Natural killer cells: development, maturation, and clinical utilization, Front. Immunol. 9 (2018) 1869, https://doi.org/10.3389/fimmu.2018.01869.
[19] V. Béziat, et al., CD56brightCD16+ NK cells: a functional intermediate stage of NK cell differentiation, J. Immunol. 186 (12) (2011) 6753–6761, https://doi.org/10.4049/jimmunol.1100330.
[20] Z. Ghazvinian, et al., Chemo-immune cell therapy by intratumoral injection of adoptive NK cells with capecitabine in gastric cancer xenograft model, Bioimpacts 13 (5) (2023) 383–392, https://doi.org/10.34172/bi.2022.26386.
[21] J.P. Veluchamy, et al., Standardized and flexible eight colour flow cytometry panels harmonized between different laboratories to study human NK cell phenotype and function, Sci. Rep. 7 (2017), 43873, https://doi.org/10.1038/srep43873.
[22] Genentech, Prescriber Information, 2021. https://www.gene.com/download/pdf/rituxan_prescribing.pdf.
[23] Y. Jing, et al., Identification of an ADAM17 cleavage region in human CD16 (FcγRIII) and the engineering of a non-cleavable version of the receptor in NK cells, PLoS One 10 (3) (2015), e0121788, https://doi.org/10.1371/journal.pone.0121788.
[24] K. Srpan, et al., Shedding of CD16 disassembles the NK cell immune synapse and boosts serial engagement of target cells, J. Cell Biol. 217 (9) (2018) 3267–3283, https://doi.org/10.1083/jcb.201712085.
[25] Y. Wang, et al., ADAM17 cleaves CD16b (FcγRIIIb) in human neutrophils, Biochim. Biophys. Acta 1833 (3) (2013) 680–685, https://doi.org/10.1016/j.bbamcr.2012.11.027.

[26] S.S. Somanchi, et al., A novel method for assessment of natural killer cell cytotoxicity using image cytometry, PLoS One 10 (10) (2015), e0141074, https://doi.org/10.1371/journal.pone.0141074.
[27] C. Hage, et al., Sorafenib induces pyroptosis in macrophages and triggers natural killer cell-mediated cytotoxicity against hepatocellular carcinoma, Hepatology 70 (4) (2019) 1280–1297, https://doi.org/10.1002/hep.30666.
[28] K. Kaur, et al., ADCC against MICA/B is mediated against differentiated oral and pancreatic and not stem-like/poorly differentiated tumors by the NK cells; loss in cancer patients due to down-modulation of CD16 receptor, Cancers 13 (2) (2021), https://doi.org/10.3390/cancers13020239.
[29] Z. Mazorra, et al., Nimotuzumab induces NK cell activation, cytotoxicity, dendritic cell maturation and expansion of EGFR-specific T cells in head and neck cancer patients, Front. Pharmacol. 8 (2017) 382, https://doi.org/10.3389/fphar.2017.00382.